

Effect of Spatial Scale on Soil Moisture Retrieval From Passive Microwave Sensors

Pancier, R.¹, J. P. Walker¹, E. Kim², J. Kalma³ and O. Merlin¹

¹Department of Civil and Environmental Engineering, The University of Melbourne, Australia

²Hydrospheric and Biospheric Sciences Lab, NASA Goddard Space Flight Center, USA

³School of Engineering, The University of Newcastle, Australia

Email: rocco@civenv.unimelb.edu.au

Keywords: Remote sensing, passive microwave, soil moisture, scaling

EXTENDED ABSTRACT

Near-surface soil moisture (SM) retrieval from L-band (1.4 GHz) passive microwave brightness temperature (T_B) measurements has been demonstrated from tower and airborne experiments (Wang 1983, Jackson et al. 1999). Current passive microwave techniques for SM retrieval are based on inversion of radiative transfer models which simulate the microwave emission from the earth surface given a specified soil water content, soil temperature, vegetation water content, surface roughness, and so on. These models assume homogeneous conditions within each pixel, and have been developed from radiometer data of homogenous pixels with resolutions on the order of 10's of meters. However, the strong non-linearity that exists in such models with respect to land surface parameters (i.e., vegetation and soil moisture), stems the question whether the same model should be applied to heterogeneous pixels at satellite footprint scales (~40km), where the land surface heterogeneity is expected to be significant. As shown in figure 1, even in the simple case of a smooth, non-vegetated surface, the non-linearity would imply that the field average SM retrieved from a single low resolution footprint is different than that calculated by averaging the SM retrieved from high resolution pixels over the same area.

This study examines the impact of land surface heterogeneity that typically exists in low resolution satellite data and the effect of non-linearity between T_B and SM. This will be done making use of independent multiple resolution L-band passive microwave aircraft observations of the same area which were collected during an extensive field campaign; the National Airborne Field Experiment (NAFE) conducted in Australia in 2005. The range of resolutions analyzed extends from 10's meters to 1 kilometer. The observations were acquired by flying an L-band radiometer over the same ground location at different altitudes. Concurrent ground

monitoring of soil moisture and other relevant data allowed detailed characterization of the land surface conditions. First, this study shows that the T_B data collected at high resolution can be averaged to low resolution, with a specific focus on two large heterogeneous areas and with the scope of verifying that satellite scale pixels can be simulated by linearly aggregating aircraft pixels of higher resolution, as this is a major assumption in synthetic satellite verification and scaling studies. Second, this study demonstrates using field data the problem of applying tower-based algorithms to heterogeneous pixels. To this end, T_B observations at two different resolutions (90m and 1km) are compared with highly detailed ground measurement of SM. Results are discussed with reference to the land surface heterogeneity at the sites, showing that care is required in retrieving soil moisture from passive microwave observations over heterogeneous areas.

This study is unique in that it makes use of T_B observations collected by the same sensor at different resolutions and supported by ground monitoring of the land surface at sub-pixel scale for all resolutions.

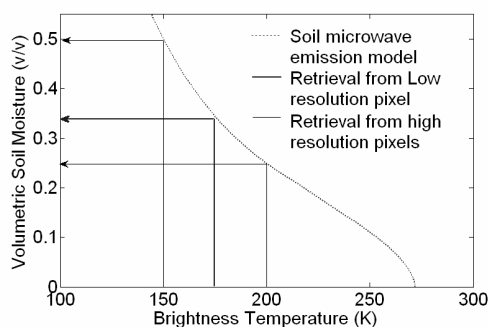


Figure 1. The problem of low resolution soil moisture retrieval for a simple case of a smooth bare, silty loam soil at 299K temperature

1. INTRODUCTION

The efficient monitoring of soil moisture (SM) has intrinsic problems, mainly associated with the fact that it exhibits a continuous spectrum of temporal and spatial scales, ranging from centimeters to thousands of kilometers and from minutes to several months (Rodriguez-Iturbe et al. 1995). Hence there are severe limitations on traditional ground-based “point” measurements which have little support and large spacing. Remote sensing has a unique potential for providing frequent observations of SM over large regions, as it overcomes the intrinsic problems of traditional ground based point measurement by providing an area averaged value of SM (Schmugge et al. 1980). Moreover, numerous studies conducted in the past two decades with microwave radiometers have shown L-band (21 cm, 1.4 GHz) measurements to be a very effective observation wavelength for SM retrieval, due to the greater depths at which information on the SM profile is retrieved and the moderate effect of vegetation and surface roughness (Jackson et al. 1984, Wang 1983). Based on these studies, SM retrieval algorithms have been developed from tower mounted radiometers. While such algorithms include the effects of vegetation cover and surface roughness, and have been tested successfully during extensive ground and airborne field experiments, such as the Washita’92 and Southern Great Plains’97 (Jackson et al. 1999), they do not account for the landscape heterogeneity that exists at satellite footprint scale.

The upcoming launch of ESA’s Soil Moisture and Ocean Salinity (SMOS) mission will provide the first dedicated L-band global data set for SM. The mission will carry a 2D interferometric radiometer, operating at L-band with V and H polarised observations at a range of incidence angles (Kerr et al. 2001). The utilisation of this novel technique on a space-borne platform poses several scientific questions yet to be answered. In particular, applicability of the L-band SM retrieval algorithms developed from effectively homogeneous point measurements to large (~40km for SMOS) heterogeneous scenes.

This issue has had limited attention to date and is the focus of this paper. Due to the lack of L-band space-borne data, as well as that of concurrent multiple resolution L-band observations, previous studies on this topic have relied on the simulation of synthetic coarse scale pixels through radiative transfer and land surface models (e.g., Burke et al. 2004). Very few studies have made use of observations to explore this issue. Amongst these, Jackson (2001) compared for the first time a limited number of independent T_B observation at

resolutions ranging from 100m to 1km. His results showed that the same average T_B was observed at different resolutions over the study area. Moreover, he explored the relationship of T_B with ground measurements of SM, finding that the same relationship could be applied at all resolutions. However, his results are limited to V polarised T_B , which are not optimal for SM retrieval, and the data covered only a small range of soil wetness conditions and land cover types (winter wheat and pasture). While the present study addresses the same problem, it is unique in that it makes use of an extensive dataset of H polarised T_B data at native resolutions ranging from 30m to 1.5km, collected by the same sensor over a full range of wetness conditions and variety of land cover types, including a range of crops, native pasture and forested areas.

2. EXPERIMENT DESCRIPTION

The multi-resolution T_B observations and ground data used in this study were collected during the National Airborne Field Experiment (NAFE) conducted during November 2005 in the Goulburn River catchment, located in a semiarid area of South-Eastern Australia. The campaign included extensive airborne passive microwave observations together with spatially distributed and in-situ ground monitoring of SM, vegetation water content (VWC), soil temperature and other relevant land surface characteristics. Full details about the field campaign and the data collected can be found elsewhere (see Walker et al., this issue). Only the ground and airborne data relevant to this analysis are described here.

2.1. Ground Data

The area monitored during NAFE’05 was an approximately 40km x 40km region, centred in the northern part of the Goulburn catchment. This area was logistically divided into two focus areas, the “Merriwa” area in the eastern part of the catchment and the “Krui” area in the western part. The general layout of the two focus areas is shown in Figure 2. The predominant land use is grazing on native pasture followed by open woodland. A considerable fraction of the area is used for cropping, including mainly wheat, barley and lucerne, with small amounts of sorghum and oats. While the Krui area is fairly uniform throughout and dominated by native pasture and crops, the Merriwa area is more heterogeneous with a large fraction of open woodland areas.

Eight farms were accessible for ground sampling and are indicated in figure 2 (the name code references to Table 1). Each farm contained a

small “high resolution” (HR) area of 150m x 150m for detailed ground sampling of soil moisture, soil temperature and VWC. The HR areas were selected to include a variety of land cover, topography and other defining features as summarised in Table 1. Top 5 cm SM was monitored at each HR area on a 12.5m grid, with a core of 75m x 75m sampled on a 6.25m grid. The surrounding areas were sampled at decreasing resolutions of 62.5m, 125m, 250m and 500m to the extremity of the farm (64km² in one instance; P). Each farm was sampled once a week, concurrently with multiple resolution aircraft observations over the area. VWC was sampled by taking biomass samples at 16 locations within the HR area and at least 6 locations across the farm once a week. The range of VWC experienced by each HR area during the campaign is given in Table 1, together with the average spatial standard deviation. Near surface SM and top soil temperature were also continuously monitored at each farm, in most cases within 1km from the HR area.

2.2. Polarimetric L-band Multi-beam Radiometer Data

A total of 16 multi-resolution flights were conducted between October 31 and November 25. This flight type was conducted from Tuesday to Friday, alternatively over the Merriwa and Krui focus areas. The passive microwave instrument used was the Polarimetric L-band Multi-beam Radiometer (PLMR). The PLMR measured both V and H polarised T_B at incidence angles $\pm 7^\circ$, $\pm 21.5^\circ$ and $\pm 38.5^\circ$ across-track. The focus area was covered with parallel, north-south oriented flight lines, each overlapping by at least 1 full pixel.

For each flight, microwave observations were collected at 4 different altitudes in descending order (3000m, 1500m, ~750m and ~200m AGL), resulting in L-band maps at nominally 1km (low), 500m (medium), 250m (high) and 62.5m (very high) spatial resolutions (figure 2). However, the

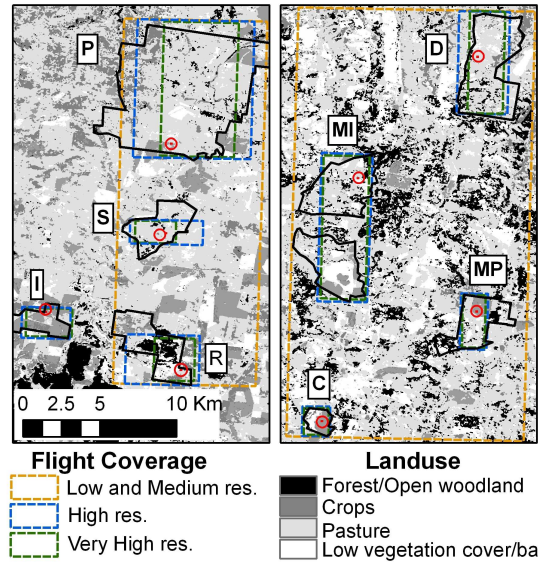


Figure 2. Krui (left) and Merriwa (right) focus areas; the 8 HR focus areas are indicated in red circles and the name code is given in Table 1.

actual resolution achieved varies across the flight coverage due to variations in terrain elevation (Table 2, column 5); hereby the actual resolution will be used to identify the observations at different resolutions. To avoid data gaps due to pixel size variations, particularly significant for the two lower altitude flights, flight altitudes were varied slightly for each farm to yield the nominal pixel resolution at the farms maximum terrain elevation.

2.3. Data Processing

The PLMR was calibrated daily against ground targets. Complete details about the calibration procedures are given in Panciera et al. (2007). The accuracy was estimated to be better than 0.7K at H polarisation and 2K for V polarisation. This study focuses on H polarised data, as they have been shown to be most sensitive to SM. The calibrated radiometer data were geometrically corrected for aircraft pitch, roll, and yaw, and the beam centers

Table 1. Location and characteristics of the High Resolution (HR) areas. Standard deviations of SM and VWC for each HR area is the average of 4 sampling dates.

HR area	land cover	Standard deviation of SM (%v/v)	VWC [Kg/m ²] (min-max)	Standard deviation of VWC [Kg/m ²]	Roughness RMS height (cm)	% sand	% clay
Stanley(S)	Native	6.5	0.1-0.4	0.1	1.07	6	54
Roscommon(R)	Native	3.5	0.2-1.1	0.3	0.62	67	15
Dales (D)	Native	8.0	0.2-0.8	0.2	0.89	31	51
Merriwa Park (MP)	Wheat	7.3	0.6-2.0	0.6	0.63	21	36
Midlothian (MI)	Fallow/Lucerne	8.1	0.1-1.3	0.2	0.82	10	69
Cullingral (C)	Wheat/Barley	5.2	0.4-1.1	0.4	0.65	72	6
Illogan (I)	Oats/Barley	7.5	0.3-2.1	0.8	0.97	23	26
Pembroke (P)	Wheat/Barley	6.1	0.5-2.7	0.9	0.84	6	71

Table 2. Characteristics of the multi-resolution flights during NAFE'05.

Flight	Nominal Altitude (m AGL)	Average Start Time (local)	Average End Time (local)	Footprint Dimension at 3dB (m)			
				Mean	Stdev	Min	Max
Low resolution (L)	3000	7:21 AM	7:40 AM	1000	105	767	1623
Medium resolution (M)	1500	7:44 AM	8:30 AM	500	68	375	958
High resolution (H)	750	8:34 AM	8:53 AM	300	37	186	568
Very high resolution (VH)	200	9:17 AM	11:13 AM	90	14	32	255

projected onto a 250m digital elevation model of the study area to provide beam centers together with the local incidence angle and effective footprint size.

All data have been normalised to an equivalent nadir T_B due to angular variations across the flight track, yielding T_B maps which are comparable across resolutions. This normalisation procedure used the assumption of previous studies (Jackson, 2001), that the deviation of average T_B measured by different beams on each day over the entire area is due mainly to the Fresnel effect, and that this effect is constant on each day for the range of vegetation and soil moisture of the area. This assumption has limitations when used in conjunction with limited data sets, but in the present case it is well founded due to the large number of data points. A beam correction coefficient was therefore calculated for each beam as the ratio of average nadir T_B , calculated as the mean between the two close-to-nadir beams, to the average T_B for the beam of interest. The resulting data set consists of nadir-referenced L-band maps for 16 dates, with 8 for each of the Merriwa and Krui focus areas, and 4 resolutions per date.

3. RESULTS AND DISCUSSIONS

To analyse the effect of resolution on the relationship between T_B and SM, first the scaling properties of the T_B fields over the Krui and Merriwa focus areas were analysed. The relationship between T_B and SM was then explored using the ground SM data and T_B observations over the HR areas.

3.1. Scaling of Brightness Temperatures

Here we investigate the effect of the sensor resolution on spatial structure and mean intensity of the T_B signal observed over the two focus areas. This analysis includes comparison of the area-averaged T_B measured at different resolutions over the focus areas as well as individual footprint comparison of the T_B measured at different resolutions.

An example of the resulting multi-resolution maps is shown in Figure 3 for November 1, a very wet

day. The geolocated and nadir-referenced data were linearly averaged to a regular grid with pixel size equivalent to the mean spatial resolution for each altitude (Table 2). The consistency between patterns of T_B at different resolutions is notable. These patterns are well defined in the 90m data and still observed in the 1km data, although the gradients are smoother. The images show how the main spatial features of T_B distribution are retained as the resolution of observation decreases, although generalised and smoothed. The average T_B for each of the 4 resolutions as displayed in Figure 3, has been computed for each of the two focus areas on a daily basis. Results are shown for the Krui focus area in Figure 4a, limited to the 1km and 90m data (results for intermediate resolution data fall within these values). Also plotted is the standard deviation across the area for both data sets. It is shown that over the full range of wetness conditions (nearly saturated at the beginning of the month to very dry at the end), there are no significant differences between the area-averaged T_B for different spatial resolutions. The absolute error between the two is consistently inferior to 5K and doesn't show any particular correlation with the overall wetness conditions. The standard deviation of the T_B fields instead is higher on wet conditions and decreases during drying down period. Moreover, it is consistently higher for 90m data than for 1km data. This is expected, as 90m data are able to resolve finer spatial details resulting from heterogeneity.

The effect of resolution on the area-averaged T_B is shown for all sampling dates and both areas in

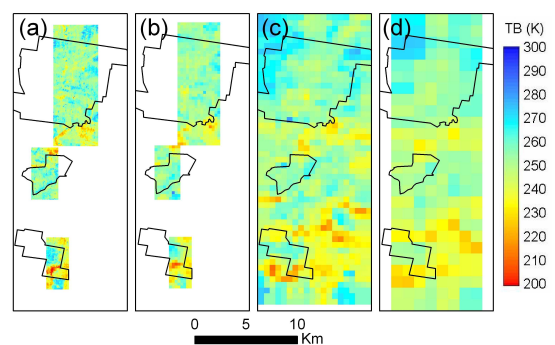


Figure 3. Example of multi-resolution T_B for the Krui area on November 1. Maps are for data at: a) 90m; b) 300m; c) 500m and d) 1km resolution.

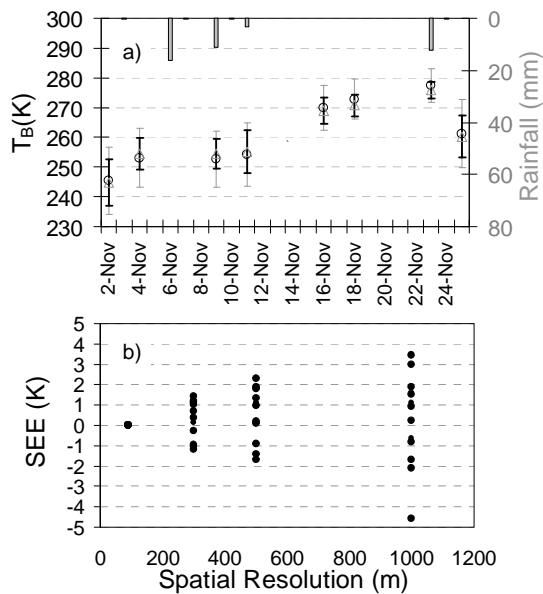


Figure 4. a) Temporal variation of the average T_B over the Krui area for 1km (black circles) and 90m (gray triangles) data; b) Effect of resolution on the Standard Error of Estimate both focus areas.

Figure 4b. To quantify this difference we use the Standard Error of Estimate (SEE), defined as the absolute error between the area-averaged T_B of low resolution data (respectively 1km, 500m and 300m) and the area-average T_B of high resolution (90m) data. By definition, the SEE for 90m data is zero. The plot shows a general increase of SEE as the resolution is decreased, but overall the SEE out to 1km resolution is insignificant, with 3K representing only ~1% v/v soil moisture content change. Considering an instrument noise of approximately 1K, this error reduces to less than 1K for the vast majority of days considered in Figure 4b. The uniform distribution across the y-axis also indicates no bias in the use of a particular resolution. Note that the increase in SEE has a similar magnitude between the 90m and 300m data and the 300m and 500m data, and only a minimal increase between the 500m and 1km data. This supports the extrapolation of these results to satellite footprint scales.

Comparison of individual footprints was undertaken by considering each low resolution footprint (1km, 500m and 300m data) and the corresponding high resolution footprints falling entirely within it. The low resolution T_B was compared with the average T_B value of the high resolution footprints in terms of SEE. The cumulated frequency distribution of this SEE is shown in Figure 5. Note that this plot includes data over the entire Krui and Merriwa area for all mapping dates, and therefore encompasses a very wide range of land surface conditions and a full range of wetness states. More than 80% of the SEE

values are contained within the +/- 3K band, with a standard deviation of 3.2K and 3.4K for Krui and Merriwa respectively. Detailed analysis revealed that higher SEE are mainly associated with unusually high heterogeneity of the high resolution T_B within the low resolution pixel. For example, a steep soil moisture gradient provoked by localised showers.

The analysis presented shows that averaging of T_B measurements at high resolution to a lower resolution results in a good agreement with the direct lower resolution measurements. Although the lowest resolution considered in this analysis was 1km, the results suggest that aircraft data can be reliably averaged up to satellite footprint resolutions for the purpose of synthetic satellite scaling studies and satellite verification when that data becomes available.

3.2. Brightness Temperatures and Soil Moisture Relationships

The relationship between T_B and SM and its variation with resolution was analysed with a focus on the HR areas at the 8 focus farms. These areas were chosen to represent a range of land surface conditions potentially contributing to variation in microwave emission. For each HR area and each day when ground sampling and aircraft mapping was undertaken, T_B footprints covering the HR area were extracted for the highest resolution data (90m) and averaged into one T_B observation. Similarly, the lowest resolution (1km) footprint containing the HR area was selected. A concurrent value of ground SM was calculated for each footprint by averaging all the ground measurements falling within it. Before making comparison with soil moisture, it was necessary to normalise the observed brightness temperature with the physical temperature of the emitting layer. This was particularly important due to (i) the daily time lag between 1km and 90m observations and (ii) the different acquisition days resulting in

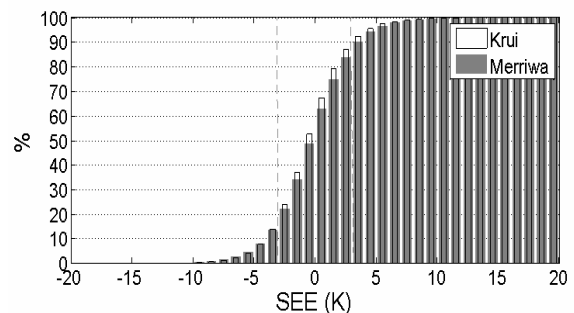


Figure 5. Cumulated frequency distribution of the footprint-by-footprint SEE between low (1km, 500m and 300m) and high (90m) resolution data. Orange dotted lines indicate the reference +/-3K limit.

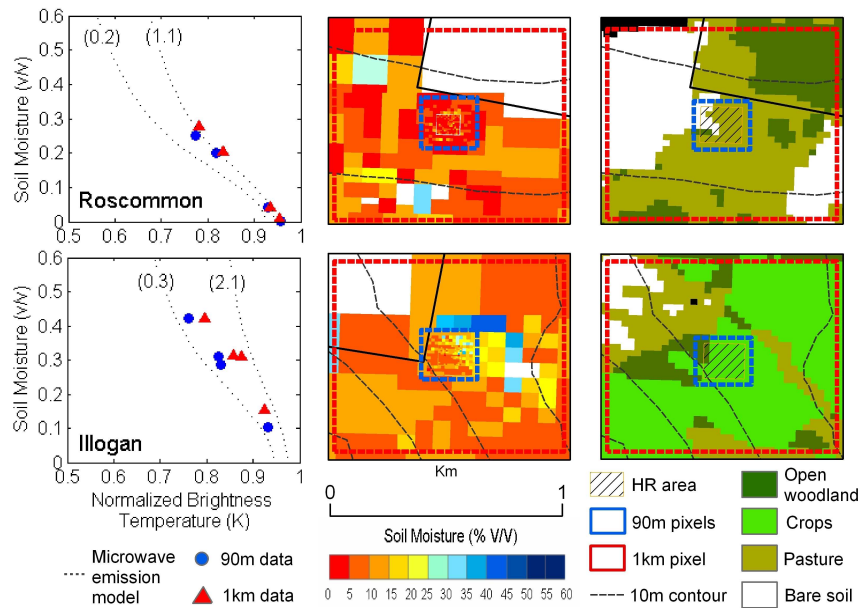


Figure 6. Effect of resolution on the relationship between T_B observations and ground SM (left panels), example of measured ground SM patterns (middle panels) and Landsat-derived land cover map (right panels) for the Roscommon (top) and Illogan (bottom) sites. Brackets in the left panels indicate the VWC used in the respective model simulation

changes in physical temperature in the soil and vegetation (see Table 2). T_B was therefore normalised using the value of the top 5 cm soil temperature recorded at the nearby monitoring station at the time of the T_B acquisition. The difference between the soil temperature recorded at the station and that recorded at various locations around the farm was found to be less than 2K, resulting in an error in estimated emissivity (assuming bare soil) less than 0.01. It is important to highlight that the comparison here is made between the relationship of T_B observed at different resolutions and the concurrent ground SM and not between the T_B /SM data points acquired on the same day. These are not directly comparable, as the 1km data cover a much larger area than the HR area while the 90m pixels are limited to the HR area.

The results in terms of normalised T_B versus SM are plotted in Figure 6 for the 90m and 1km resolution footprints. An example of a homogenous and heterogenous pixel is given in the top panel ('Roscommon'). Also plotted is the relationship between T_B and SM simulated by the microwave emission model using uniform soil, vegetation and surface roughness parameters recorded at the HR area (dotted lines). The simulations correspond to the maximum and the minimum VWC recorded at the HR area, and show a good match with observed data. All the data points fall within the region delimited by the low and high VWC simulations (the actual position of the data point depends on the VWC on the day).

The microwave emission model used is therefore consistent with both the 90m and 1km resolution data, but the bottom panel shows that a different relationship exists between T_B and SM at the two different resolutions.

As shown in the middle and right panels of figure 6, the Roscommon site presents fairly uniform land surface conditions, flat topography and mainly uniform very short native grass or nearly bare soil, resulting in relatively uniform SM field (average standard deviation of 3.5%v/v for the 1km footprint). The soil type at the site was characterised with several soil textural samples and found to be very homogeneous. In contrast, the Illogan site is quite heterogeneous, being situated in a valley bottom and presenting a variety of land covers including, crops, native grass and areas of open woodland, which reflect in the high standard deviation of both VWC (0.8Kg.m^{-2}) and SM (7.5%v/v). The effect of these different land surface conditions on the relationship between normalised T_B and SM is shown in the left panels of Figure 6. While the Roscommon site displays the same relationship at 90m and 1km resolutions, a different relationship exists at different resolutions in the case of Illogan. This is due to the greater heterogeneity in SM and VWC of the Illogan site.

4. CONCLUSIONS

In this study, multiple resolution L-band T_B observations and concurrent ground data were used

to examine the implications of land surface heterogeneity on soil moisture retrieval when working with low resolution satellite data. It was shown that in the absence of actual L-band satellite observations, synthetic satellite footprints can be simulated by simple linear aggregation of aircraft footprints. The error in retrieved SM due to this operation is expected to be less than 1% v/v. It was also shown that the resolution of the observed T_B has a detectable effect on the relationship between T_B and SM in the case of heterogeneous land surface conditions within the sensor field of view, which is expected to be significant at the satellite footprint scale. The implication of these results for SM retrieval from satellite scale footprints will be the next step of this analysis. This will involve using the microwave emission model tested in this study to retrieve SM from a synthetic 40km pixel obtained by aggregation of the 1km observations. This SM value will then compared with the retrieved soil moisture fields from 1km data.

5. ACKNOWLEDGEMENTS

NAFE'05 has been made possible through recent infrastructure (LE0453434 and LE0560930) and research (DP0557543, DP0556941) funding from the Australian Research Council. Initial setup and maintenance of the study catchments was funded by research grants (DP0209724 and DP0556941) from the Australian Research Council and NASA. The authors also wish to thank all the components of the ground and air crew of NAFE'05.

6. REFERENCES

- Burke, E.J., W.J. Shuttleworth and P.R. Houser (2004), Impact of horizontal and vertical heterogeneities on retrievals using multiangle microwave brightness temperature data, *Geoscience and Remote Sensing, IEEE Transactions on*, 42(7), 1495.
- Jackson, T. (2001), Multiple Resolution Analysis of L-Band Brightness Temperature for Soil Moisture, *Ieee Transactions on Geoscience and Remote Sensing*, 39(1), 151-164.
- Jackson, T.J., T.J. Schmugge and J.R. Wang (1982), Passive Microwave Sensing of Soil-Moisture under Vegetation Canopies, *Water Resources Research*, 18(4), 1137-1142.
- Jackson, T.J., T.J. Schmugge and P. O'Neill (1984), Passive microwave remote sensing of soil moisture from an aircraft platform, *Remote Sensing of Environment*, 14(1-3), 135-151.
- Jackson, T.J., D.M. Le Vine, A.Y. Hsu, A. Oldak, P.J. Starks, C.T. Swift, J.D. Isham and M. Haken (1999), Soil moisture mapping at regional scales using microwave radiometry: The Southern Great Plains Hydrology Experiment, *Ieee Transactions on Geoscience and Remote Sensing*, 37(5), 2136-2151.
- Kerr, Y.H., P. Waldteufel, J.P. Wigneron, J.M. Martinuzzi, J. Font and M. Berger (2001), Soil moisture retrieval from space: The Soil Moisture and Ocean Salinity (SMOS) mission, *Ieee Transactions on Geoscience and Remote Sensing*, 39(8), 1729-1735.
- Rodriguez-Iturbe, I., G.K. Vogel, R. Rigon, D. Entekhabi, F. Castelli and A. Rinaldo (1995), On the spatial organization of soil moisture fields, *Geophysical Research Letters*, 22(20), 2757-2760.
- Schmugge, T.J., T.J. Jackson and H.L. McKim (1980), Survey of Methods for Soil Moisture determination, *Water Resources Research*, 16(6), 961-979.
- Walker, J.P., E. Botha, G. Boulet, J. Balling, M. Bell, A. Berg, M. Berger, D. Biazoni, Y. Chen, E. Christen, R. deJeu, P. deRosnay, C. Dever, C. Draper, J. Fenollar, C. Gomez, J. Grant, J. Hacker, M. Hafeez, G. Hancock, D. Hansen, L. Holz, J. Hornbuckle, R. Hurkmans, T. Jackson, J. Johanson, P. Jones, S. Jones, J. Kalma, Y. Kerr, E. Kim, V. Kuzmin, V. Lakshmi, E. Lopez, V. Maggioni, P. Maisongrande, C. Martinez, L. McKee, O. Merlin, I. Mladenova, P. O'Neill, R. Panciera, V. Paruscio, R. Pipunic, W. Rawls, M. Rinaldi, C. Rudiger, P. Saco, K. Saleh, S. Savstrup-Kristensen, V. Shoemark, N. Skou, S. Soebjaerg, G. Summerell, R. Teuling, H. Thompson, M. Thyer, J. Toyra, A. Tsang, T. Wells, P. Wursteisen and R. Young (2007), The National Airborne Field Experiment Data Sets, MODSIM, This Issue.
- Wang, J.R. (1983), Passive microwave sensing of soil moisture content: The effects of soil bulk density and surface roughness, *Remote Sensing of Environment*, 13(4), 329-344.